Full-azimuth, anisotropic 3D EM inversion applied to a low-resistivity pay reservoir with well control

D. Crider, M. Scherrer, Focus Exloration LLC
T. Pham, J.J. Zach, M.A. Frenkel, EMGS Americas*

Summary

We demonstrate advances in 3D EM inversion- based subsurface imaging on a challenging target in a mature area of the Gulf of Mexico. These advances include the use of the anisotropic (ρ_v, ρ_h) cube as well as a data weight scheme which permits inversion of all azimuthal data in the 3D grid. Our inversion is based on a quasi-Newton optimization algorithm with approximate calculation of the Hessian matrix and a finite-difference time-domain forward modeler. Its capability to resolve small targets of low-resistivity pay in complex geology is confirmed by the case example presented here. A proven hydrocarbon find ($\Delta\rho$ < 5 Ωm versus background, 2 km x 2 km) is compared with well and seismic data. There is a significant improvement in resolution over previous inversions using isotropic 3D-inversion, however, due to the acquisition in deep water and lack of substantial anisotropy, the target was identified in both cases.

Introduction

The decade-long renaissance of marine CSEM surveys boosted by the pioneering work documented by, e.g., Eidesmo et al. (2002) or Bhuiyan (2009), has been driven by their successful application towards hydrocarbon exploration. Advances in hardware, operational procedures and redundant source systems permit the acquisition of well-defined and repeatable grids of seabed receivers with complex towing patterns including the acquisition of 3D grids with azimuth data. Thus, marine CSEM has been adopted by most of the industry as a method for 3D subsurface imaging which is increasingly integrated with other geophysical data: Lovatini et al. (2009), Commer and Newman (2008), Carrazone et al. (2008), Price et al. (2008), Plessix, van der Sman, 2008, Norman et al., 2008, Yuan et al. (2009), Lorenz et al. (2009).

The 3D EM workflow used in this work is centered around an iterative inversion approach with repeated computation of the gradient of a misfit function with respect to the discrete conductivity grid, $g = \partial\varepsilon/\partial\sigma$, followed by a Hessian-based update step. The gradient calculation is based on the first Born scattering approximation, as implemented in Støren et al. (2008), and is similar to the adjoint state approach used by Plessix and Mulder (2008). The finite-difference time-domain method presented by Maaø (2007) was used to generate synthetic data and gradients. The misfit function used is the L2 norm of the difference field between synthetic and recorded data:

$$\varepsilon = \sum_{s,r,\omega,F} (\text{Weight})(\vec{x}_r \mid \vec{x}_s;\omega)\left|\Delta F_i(\vec{x}_r \mid \vec{x}_s;\omega)\right|^2 \cdot$$

The Hessian matrix in the update step is approximated using a small number of past iterations in model- and gradient steps in an outer product- formulation, Zach et al. (2008a), Byrd et al. (1995), where many other inversion approaches rely on the conjugate gradient method, e.g., Gribenko and Zhdanov (2007).

The importance of anisotropy, particularly for azimuthal data in 3D surveys, has been pointed out by Jing et al. (2008). Especially in environments with high anisotropy such as the Barents Sea, where large ratios of ρ_v/ρ_h=5-10 or more can be observed, a meaningful interpretation of even 2D surveys is not possible without taking into account anisotropy, see Nguyen et al. (2009). A potential problem which needs to be settled is the value of past isotropic inversions and interpretations of CSEM surveys. Over the past years, the industry has inverted many hundred datasets, and the vast majority has still been interpreted either assuming constant or no anisotropy. Fortunately, most areas where CSEM has been commercially applied exhibit far lower anisotropy ratios than the Barents Sea. We have therefore decided to revisit a dataset inverted with the assumption of complete isotropy, see Yuan et al. (2009), and which was acquired in an area of the Gulf of Mexico with moderate anisotropy (ρ_v/ρ_h~1.5). Furthermore, we consider the target, a proven hydrocarbon find with a lateral extent of 2 km, to represent a benchmark case for the lower end of the spectrum of meaningful CSEM targets. Besides anisotropy, we have applied other key improvements in preprocessing and inversion, which are summarized in the following.

Methodology

A summary of the technical improvements in the inversion methodology beyond follows:

1) Anisotropy: the 3D inversion is TIV anisotropic. Anisotropic constraints can be imposed through regularization, but for illustrative purposes, the anisotropy factor is not constrained in the example shown below.

2) Pre-processing: data conditioning follows largely Zach et al. (2008b), with the exception of the data-driven determination of the rotation angle. The new workflow relies on a combination of optimizations using both inline and broadside data, augmented by an inversion-based method. Greater reliability and accuracy derives mainly

from multiple independent measurements. The underlying algorithms which permit the determination of the receiver orientation to an accuracy of 2-3 degrees are still confidential at this point.

3) Full-azimuth data: determining inversion data weights with the help of rigorous use of the propagation of different data error and noise sources which influence the various measured field components, see Morten et al. (2009):

$$1/W_F^{\,2} = \left(\Delta F^{obs}\right)^2 + \eta\left(\Delta F^{noise}\right)^2,$$

$$\Delta F^{obs}_{\frac{x}{y}} = \sqrt{\alpha^2\left(F_1^{\,2}\frac{\cos}{\sin}^{2}\varphi + F_2^{\,2}\frac{\sin}{\cos}^{2}\varphi\right) + F_{\frac{2}{1}}^{\,2}\left(\Delta\varphi\right)^2}$$

where α is the relative error in the calibration, φ is the rotation angle relative to the towline and the indices 1,2 are the non-rotated receiver axes. This approach permits to use the full azimuthal data content (within the limitations of a certain minimum signal-to-noise ratio at a given azimuth/offset configuration). In prior wide-azimuth surveys, only data within a certain aperture angle relative to the source (typically around 45 degrees, depending on the survey) were included.

Case study

The survey design was a 3D grid consisting of a total of 57 receivers in two deployments. All receivers during each deployment were acquiring during the entire time, and data from both inline and azimuthal receivers (see top panel in figure 3) were included in the inversion. In terms of usable tow-kilometers, more than 80 % of the data used were from azimuthal towlines.

The water depth in the survey area is about 1100 m, with moderately complex bathymetry. One of the targets in the prospect consists of four layers of a stacked channel-levee complex extending from 1800 m- 2000 m BSL (see figure 1), two among which exhibit a substantial response on a resistivity log, see the MWD-log in figure 2. Although the gross hydrocarbon column is 300 ft thick, the logged resistivity is only as high as 30 Ωm over less than 10 m. In light of a vertical CSEM resolution in the present case of about 100 m, and an approximate conservation of transverse resistance in the CSEM response, the actual resistive anomaly is only $\Delta\rho \sim 3$ Ωm.

The inversion relies on decoupling the modeling-from the inversion grid, which were chosen to be regular grids with $(\Delta x, \Delta y, \Delta z)$=(100m, 100m, 50m) and (200m, 200m, 50m), respectively. The three higher frequencies among the quad-peak (0.25, 0.5, 0.75, 1.0 Hz) were selected for reasons of efficiency, since the target is located at less than 1 km burial depth. Both components of the horizontal electric field were inverted.

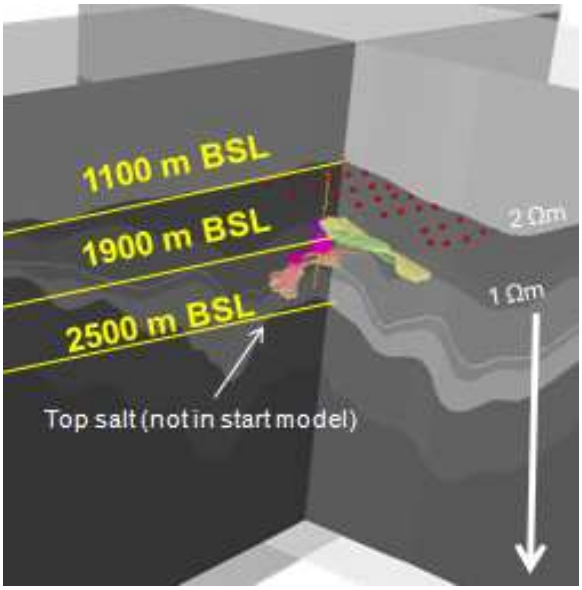

Figure 1: Main geologic horizons and proven target in the survey area. The water depth is about 1100 m, and the prospect outlines shown represent the targets based on seismic interpretation. Salt is present throughout the entire area, at a burial depth of 0.5-1.5 km.

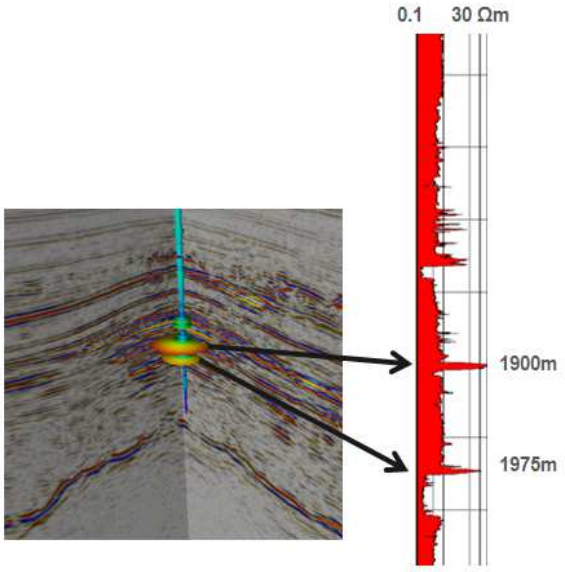

Figure 2: MWD deep-scan resistivity log of the channel-levee complex shown in figure 1. Only the two deepest channel prospects showed substantial resistivity, both at about 30 Ωm over less than 5 m. Assuming a vertical resolution of the 3D EM survey of 100 m, the anomaly is equivalent to 3 Ωm.

Full-azimuth, anisotropic 3D EM inversion applied to a low-resistivity pay reservoir with well control

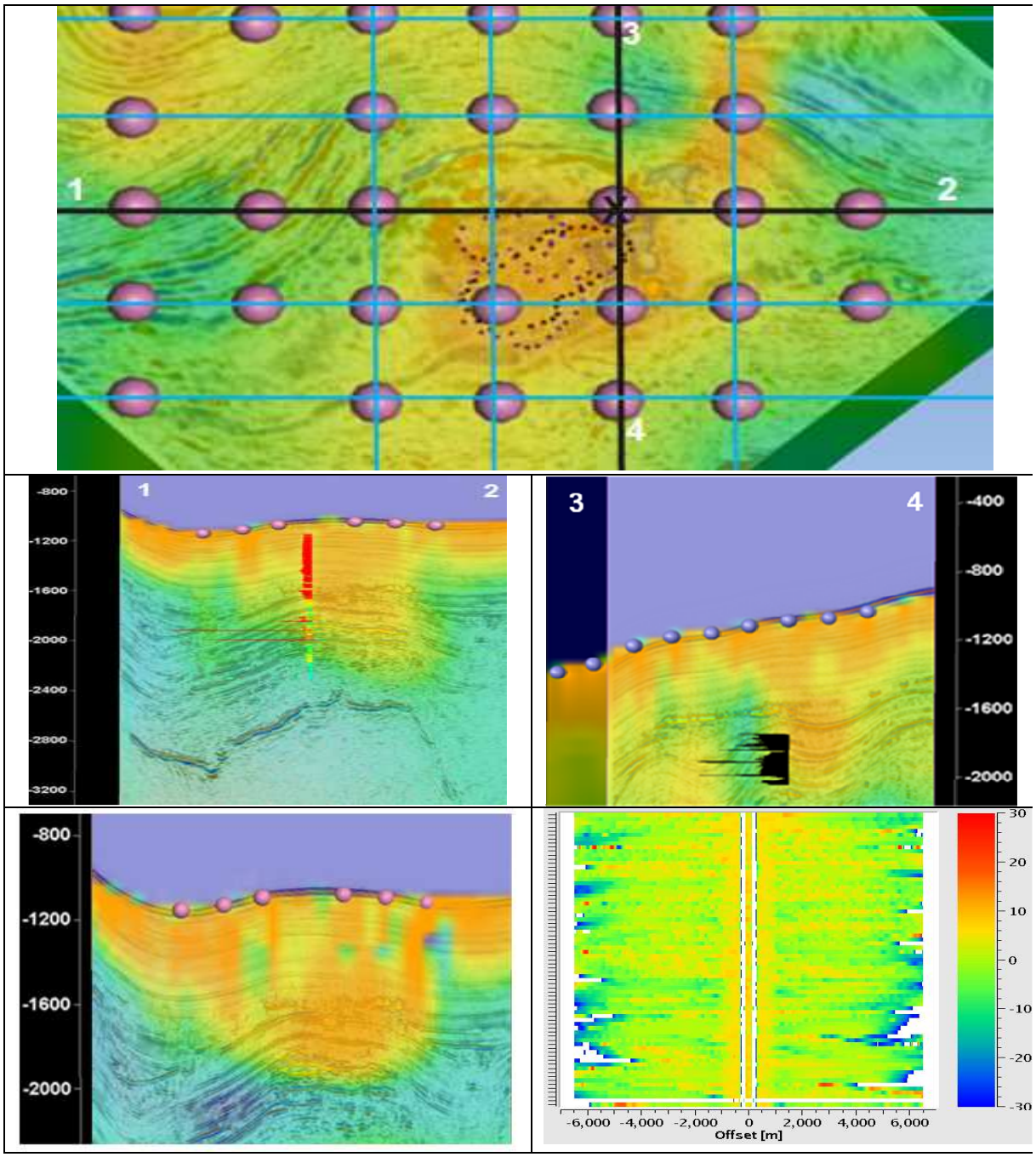

Figure 3: Result of anisotropic, full-azimuth 3D EM inversion using the frequency modes (0.5, 0.75, 1.0 Hz)- modes of both components of the horizontal electric field. Top panel: depth slice at TVD 1720 m overlaid with a seismic time slice corresponding to the same depth, showing the 3D EM anomaly in line with the seismic structure and prospect outlines. The survey design is also illustrated with the black lines being inline and the blue lines azimuthal towlines relative to the receiver marked with "X". Left/right center panel: Cross sections of the vertical resistivity component (ρ_v) of the 3D EM inversion result co-rendered with 3D seismic data along the lines "1-2"/"3-4" shown in the top panel, shown along with the MWD-log (red)/deep laterolog (black). Bottom left panel: for comparison, result of the isotropic inversion from Yuan et al. (2009), projected onto "1-2". Bottom right panel: phase misfit plot in the offset domain for the 0.5 Hz- mode; each horizontal line represents one receiver. Only the inline electric component is shown.

The same start model as in Yuan et al. (2009) was used, which relied on imprinting the result of plane-layer inversions of some reference receivers onto the geological model, starting from 2 Ωm and decreasing to about 1 Ωm at a depth of 500 m. Below, a 1 Ωm halfspace was assumed. There is salt present between 500-1500 m below the target, however, this was not included in the start model, which proved not to be detrimental to recovering the target. No anisotropy was assumed in the start model.

The result of the inversion after convergence has been achieved to within 5% in magnitude and 5 degrees in phase at offset ranges relevant for the main targets is shown in figure 3. Both in terms of the number of iterations needed and the time per iteration, convergence is achieved for either the isotropic or anisotropic case within 80-200 iterations at typically one-two hours per iteration. The anisotropic inversion result exhibits a considerably better match with the outline of the structure. This is true both in terms of lateral edge detection when considering a depth section, as well as in terms of depth.

Concerning the interpretation of the result, an MWD log exists from a depth of 60m below mudline. Comprehensive log analysis, in particular the gamma-ray versus the resistivity logs, conclusively shows a shale overburden with occasional silt stringers from 60m to 630m. Compared to the sand below, this shale layer has an enhanced resistivity (ρ_h=1.5Ωm compared to ρ_h=0.7Ωm in the sand). This is confirmed by a relatively resistive shale layer with constant thickness appearing on the 3D EM inversion image throughout the entire survey. Immediately below the shale layer follows the stacked pay of the target with a resistive anomaly of effectively $\Delta\rho$~3 Ωm, which is the reason why there is no clear spatial separation between both – such resolution is not in the data, and further analysis has to be conducted by post-inversion modeling. The same is true for the resolution of stacked prospects separated by only 75 m. However, the identification of the target on the 3D EM image is still a clear case, as it comprises the only substantial resistive bulge protruding from the shale overburden.

Conclusions

Using an improved, industrialized 3D EM workflow, we have demonstrated that full azimuth data can be utilized in an anisotropic inversion to image a known reservoir in the close vicinity (a few hundred meters of stacking) of extensive salt structures. Considerable improvement in resolution can be achieved compared to an isotropic algorithm with wide-, but not full-azimuth capability.

Hundreds of CSEM surveys have been acquired over the past decade, most of which were interpreted using the isotropic approximation. The basic conclusion of the present survey, acquired in an area with no severe anisotropy, is not changed compared to isotropic inversion. This suggests that not each survey among the extensive library acquired within the industry by now will have to be completely re-interpreted.

While taking into account anisotropy is essential to obtain value from 3D EM, we still view isotropic inversion as an important quality control tool, especially in areas where no firm data exist on the expected anisotropy factor. This is due to the different depths at which a 3D EM survey is sensitive to the vertical versus the horizontal resistivity. The long-held asymptotic wisdom that CSEM measures mainly the vertical resistivity is only approximately true at burial depths small compared to the skin depth. Figure 4 shows a vertical section of the horizontal resistivity obtained in the present inversion, through the line "1-2" shown in figure 3. Since no regularization was applied to the anisotropy factor, the reservoir is not recovered in ρ_h, as opposed to the salt at greater depths showing a stronger response compared to ρ_v,. Due to this dichotomy, we stress the importance of including both vertical and horizontal resistivity in the analysis and interpretation.

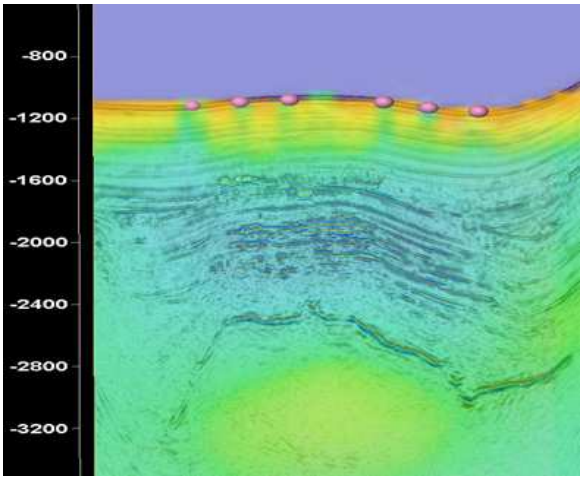

Figure 4: Horizontal resistivity section through line "1-2" resulting from the anisotropic 3D EM inversion. No a priori knowledge of anisotropy was assumed, and the lack of constraints resulted in the target to only appear in the vertical resistivity response. However, since the sensitivity to ρ_h is superior to ρ_v at greater depths, the salt response is stronger here.

Acknowledgements

We would like to thank Focus Exploration, LLC and EMGS Americas for supporting this study and permitting its publication, David Ridyard and Bjarte Bruheim for valuable discussions and the field geophysicists and crew of the M/V Siem Mollie for acquiring a high quality dataset with strict adherence to our QHSE standards.

EDITED REFERENCES

Note: This reference list is a copy-edited version of the reference list submitted by the author. Reference lists for the 2010 SEG Technical Program Expanded Abstracts have been copy edited so that references provided with the online metadata for each paper will achieve a high degree of linking to cited sources that appear on the Web.

REFERENCES

Bhuiyan, A. H., 2009, Three-dimensional modelling and interpretation of CSEM data from offshore Angola: Petroleum Geoscience, **15**, 175–189, doi:10.1144/1354-079309-803.

Byrd, R. H., P. Lu, J. Nocedal, and C. Zhu, 1995, A Limited Memory Algorithm for Bound Constrained Optimization: SIAM Journal on Scientific and Statistical Computing, **16**, no. 5, 1190–1208, doi:10.1137/0916069.

Carrazone, J. J., T. A. Dickens, K. E. Green, C. Jing, L. A. Wahrmund, D. E. Willen, M. Commer, and G. A. Newman, 2008, Inversion study of a large marine CSEM survey: 78th Annual international meeting, SEG, Expanded Abstracts, **27**, 644.

Commer, M., and G. A. Newman, 2008, Optimal conductivity reconstruction using three-dimensional joint and model-based inversion for controlled-source and magnetotelluric data: 78th Annual international meeting, SEG, Expanded Abstracts, **27**, no. 1, 609, doi:10.1190/1.3063725.

Eidesmo, T., S. Ellingsrud, L. M. MacGregor, S. Constable, M. C. Sinha, S. Johansen, F. N. Kong, and H. Westerdahl, 2002, Sea Bed Logging (SBL), a new method for remote and direct identification of hydrocarbon filled layers in deepwater areas: First Break, **20**, 144–152.

Gribenko, A., and M. Zhdanov, 2007, Rigorous 3D inversion of marine CSEM data based on the integral equation method: Geophysics, **72**, no. 2, WA73–WA84, doi:10.1190/1.2435712.

Jing, C., K. E. Green, and D. E. Willen, 2008, CSEM inversion: Impact of anisotropy, data coverage, and initial models: 78th Annual international meeting, SEG, Expanded Abstracts, **27**, no. 1, 604, doi:10.1190/1.3063724.

Lorenz, L., H. Pedersen, M. Akella, A. Tyagi, P. Sangvai, and R. Bastia, 2009, Interpreting SBL data in complex resistivity regime; integration of advanced EM-techniques with existing geophysical exploration data: 79th Annual international meeting, SEG, Expanded Abstracts, **28**, 840.

Lovatini, A., M. D. Watts, K. E. Umbach, A. Ferster, S. Patmore, and J. Stilling, 2009, Application of 3D anisotropic CSEM inversion offshore west of Greenland: 79th Annual international meeting, SEG, Expanded Abstracts, **28**, 830.

Maaø, F. A., 2007, Fast finite-difference time-domain modeling of marine-subsurface electromagnetic problems: Geophysics, **72**, no. 2, A19–A23. doi:10.1190/1.2434781

Morten, J. P., A. K. Bjørke, and T. Støren, 2009, CSEM data uncertainty analysis for 3D inversion: 79th Annual international meeting, SEG, Expanded Abstracts, **28**, 724.

Nguyen, A. K., S. Fanavoll, K. R. Hansen, J. P. Morten, and R. Tharimela, 2009, EM anomaly detection under a high resistive, anisotropic overburden: Inversion study from the Nucula discovery, Barents Sea: Geological Society of Norway conference: "Recent advances in interpretation of geophysical data 2009, EM - An Emerging Technology in Petroleum Exploration.

Norman, T., H. Alnes, O. Christensen, J. J. Zach, O. Eiken, E. Tjåland, 2008 Planning Time-lapse CSEM-surveys for Joint Seismic-EM Monitoring of Geological Carbon Dioxide Injection: First EAGE CO2 Geoogical Storage Workshop, EAGE, Expanded Abstracts A11.

Plessix, R.-E., and P. van der Sman, 2008, Regularized and blocky controlled source electromagnetic inversion: PIERS Online, **4**, no. 7, 755–760, doi:10.2529/PIERS071129160624

Plessix, R.-E., Mulder, W.A. (2008) Resistivity imaging with controlled-source electromagnetic data: depth and data weighting: Inverse Problems 24, 034012.

Price, A., P. Turpin, M. Erbetta, D. Watts, and G. Cairns, 2008, 1D, 2D and 3D modeling and inversion of 3D CSEM data offshore West Africa: 78th Annual international meeting, SEG: Expanded Abstracts, **27**, no. 1, 639, doi:10.1190/1.3063732.

Støren, T., J. J. Zach, and F. Maaø, 2008, Gradient calculations for 3D inversion of CSEM data using a fast finite-difference time-domain modelling code: 70th EAGE Conference & Exhibitions, Expanded Abstracts, P194.

Yuan, H., T. Pham, J. J. Zach, M. A. Frenkel, and D. Ridyard, 2009, Exploration case studies in mature Gulf of Mexico basins using 3D marine CSEM: 79th Annual international meeting, SEG: Expanded Abstracts, **28**, 825.

Zach, J. J., A. K. Bjørke, T. Støren, and F. Maaø, 2008a, 3D inversion of marine CSEM data using a fast finite-difference time-domain forward code and approximate Hessian-based optimization: SEG Technical Program Expanded Abstracts, **27**, 614. doi:10.1190/1.3063726

Zach, J. J., F. Roth, and H. Yuan, 2008b, Data preprocessing and starting model preparation for 3D inversion of marine CSEM surveys: 70th EAGE Conference & Exhibition, Expanded Abstracts, G003.